Research article

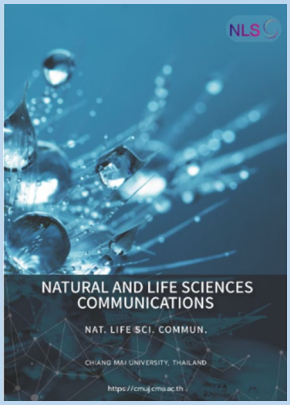

Editor:
Supon Ananta,
Chiang Mai University, Thailand

Article history:
Received: October 27, 2022;
Revised: March 30, 2023;
Accepted: April 19, 2023;
https://doi.org/10.12982/NLSC.2023.042

Corresponding author:
Munasir
E-mail: *munasir_physics@unesa.ac.id*

Green Synthesis of Fe_3O_4 Nanoparticles Using Green Betel Leaf Extract for Methylene Blue Adsorption

Khoirotin[1], Nuhaa Faaizatunnisa[2], and Munasir[1]*

1 Department of Physics, Faculty of Mathematics and Science, Universitas Negeri Surabaya, Indonesia.
2 Department of Chemistry, FASAD, Institut Teknologi Sepuluh Nopember (ITS), Surabaya, Indonesia

ABSTRACT

The synthesis of Fe_3O_4 nanoparticles has become a matter of interest because it has properties and useful applications in various fields. Using plant extracts using the green synthesis method to manufacture Fe_3O_4 nanoparticles is considered an effective, efficient, and environmentally friendly approach because it does not contain harmful chemicals. This study uses the green synthesis method to synthesize Fe_3O_4 nanoparticles from green betel leaf extract. The UV-Vis Fe_3O_4 nanoparticles showed continuous absorption at wavelengths between 300 nm and 800 nm and obtained a band gap energy of 1.87 eV. XRD analysis confirmed the crystal size of Fe_3O_4 nanoparticles (≈ 6.93 nm). The FTIR results show that functional groups from the leaf extract play a role in forming Fe_3O_4 nanoparticles, as evidenced by the presence of two Fe-O absorption bands at wave numbers 567 cm^{-1} and 482 cm^{-1}. The SEM results showed a needle-like particle shape, the HR-TEM analysis showed spherical and needle-like shapes and nanoparticles size (≈ 29.82 nm) and the EDS analysis showed that Fe and O elements indicated the dominant iron oxide content of Fe_3O_4 with levels of 73.35% and 20.88%, respectively. The magnetization curve shows that the green synthesized magnetite has ferromagnetic properties. The ferromagnetic properties of Fe_3O_4 were then applied as methylene blue adsorbent and observed using UV-Vis spectroscopy, the most effective absorption ability was at a contact time of 120 minutes with a color degradation percentage of 98.75%.

Keywords: Green synthesis, Fe_3O_4, Green betel, Adsorption, Methylene blue

Citation: Khoirotin, Faaizatunnisa, N., and Munasir 2023. Green synthesis of Fe_3O_4 nanoparticles using green betel leaf extract for methylene blue adsorption. Natural and Life Sciences Communications. 22(3): e2023042.

INTRODUCTION

Recently, research on magnetite nanoparticles has been widely developed. Nanoparticles are attractive because they have a small shape and size, a large surface volume, and new characteristics compared to large particles of bulk materials (Latha and Gowri, 2014). Synthesis of iron oxide magnetic nanoparticles are widely carried out because of its specific properties, such as superparamagnetic (Mahdavian and Mirrahimi, 2010), biocompatible (Marciello et al., 2013), biodegradable (Zhao et al., 2009), and non-toxic to humans (Zhang et al., 2013). These attractive properties cause Fe_3O_4 nanoparticles to be widely used in various applications, such as biosensors, magnetic storage media, magnetic resonance imaging (MRI), catalysts, and targeted drug delivery (Yew et al., 2016). Magnetite can also be used as an adsorbent for water contaminants because it has a large absorption capacity and can respond to magnetic fields, thus facilitating the process of separating the adsorbent from the solution. Magnetite (Fe_3O_4) is a magnetic iron oxide with an inverted spinel cubic structure with oxygen forming a closed FCC (Face Centered Cubic) package. Fe cations are located in the tetrahedral and octahedral areas. Electrons can bounce somewhere in the range of Fe^{2+} and Fe^{3+} particles at octahedral sites at room temperature, resulting in significant grade magnetite of semi-metallic materials (Verwey, 1939).

Iron oxide nanoparticles are produced in the form of magnetite, maghemite, and hematite using chemical, physical and biological methods. Nanoparticles formed in various ways show certain properties. A conventional method for preparing iron oxide nanoparticles is the coprecipitation method. Several approaches were used to synthesize Fe_3O_4 nanoparticles: the top-down method, bottom-up method, sonochemical process, hydrodynamic cavitation, microemulsion process, radiolysis, microwave, laser ablation method, and more recently through, biosynthetic methods (Latha and Gowri, 2014). Plant parts that are usually used to synthesize magnetite nanoparticles are roots, seeds, fruits, and leaves. In addition, phytochemicals play an important role in the formation of nanoparticles as a green synthesis approach for nanotechnology. Green nanotechnology has attracted a lot of attention because the process does not involve chemical compounds, so it can reduce toxic substances to restore the environment (Aksu Demirezen et al., 2019; Mahdavi et al., 2013).

Iron oxide nanoparticles synthesized from various types of plants using the green synthesis method are a new technique to overcome the limitations of conventional methods. The main advantage of this green synthesis method is that it can easily control the shape, nature, and size of the resulting nanoparticles. In this green synthesis, bio-molecules in plants act as capping and reducing agents, causing the rate of reduction and stabilization of nanoparticles to increase.

Previously, several successful studies synthesized Fe_3O_4 nanoparticles using plant extracts. For example, *Artemisia annua* leaf extract (Basavegowda et al., 2014), *Tridax procumbens* leaf extract (Patil et al., 2020), *Carica papaya* (Latha and Gowri, 2014), *Syzygiumcumini* seed extract (Venkateswarlu et al., 2014), seaweed extract (*Kappaphycusalverezi*) (Yew et al., 2016), weed leaf extract (*Imperata Cylindrica* L) (Zulaicha et al., 2020), red betel leaf extract (*Piper crocatum*) (Khaira, Ulinas, et al., 2020), and *Moringa oleifera* plant extract (Altaf et al., 2021).

Based on the literature, biochemical elements in plants such as flavonoids, polyphenols, alkaloids and terpenoids contribute as stabilizers and protective agents in the synthesis of nanoparticles (Altaf et al., 2021). Green betel (*Piper betle* L.) is an evergreen vine with shiny heart-shaped leaves. This plant from the Piperaceae family thrives throughout tropical Asia to eastern Africa. In Indonesia, green betel plants are widespread and can be found in the house's yard. Green betel plants can be found on the islands of Sumatra, Kalimantan, Java, Sulawesi, Maluku, and Papua. This plant grows in Indonesia at an altitude of 200-1000 mdpl with rainfall of about 2,250-4,750 mm/year, increases in areas with moist soil and

cool places, and is protected from direct wind exposure (Dalimarta, 2006). The results of research conducted by Rukmini (2020) phytochemical screening on green betel leaves showed the presence of alkaloids, flavonoids, polyphenols, and terpenoids that can be used as natural reducing agents and oxidizing agents in the synthesis of Fe_3O_4 nanoparticles.

The sixth point of SDGs in 2030 is to ensure that all people worldwide have fair and equitable access to clean water and proper sanitation, increase the efficiency of water and sanitation use, reduce water pollution, and increase the protection and restoration of threatened aquatic ecosystems [https://unstats.un.org]. Now the problem of water pollution is still a severe problem for all countries that must be overcome together. Research to overcome the problem of water pollution has been carried out and varied by previous researchers. These water-soluble dyes are dangerous; they may contain non-degradable and toxic heavy metals. Pollution by these dyes can come from the impact of industrialization and people's lifestyles that are not environmentally friendly. Which, in the end, will significantly impact the emergence of various environmental and health problems because it is toxic, stable, and cannot be decomposed (Agnestisia, 2017).

Magnetite has been widely used as an adsorbent for water contaminants such as western metal contaminants Cd(II) (Iconaru et al., 2016), Pb(II) (Bagbi et al., 2016), and Cr(VI) (Padmavathy et al., 2016), Arsenic (As) (Chomchoey et al., 2018), removing rhodamine B (RhB) and methyl orange (MO) (Liu et al., 2019), reactive red, congo red and acid red (Shan et al., 2014), removal of the anionic C.I. Direct Red 23 dye (Magdy et al., 2017), and Methylene blue (MB) and Safranin-O (SO)(Ghaedi et al., 2015).

Based on these considerations and to obtain an adsorbent that is quite efficient in terms of its ability, this article reports on a green synthesis and environmentally friendly method for the preparation of magnetite nanoparticles using green betel leaf extract (*Piper betle* L.) for the adsorption of organic dye methylene blue (MB).

MATERIALS AND METHODS

Materials

The materials used in this study were samples of green betel leaf, ferric chloride hexahydrate ($FeCl_3.6H_2O$), ferric chloride tetrahydrate ($FeCl_2.4H_2O$), 1 M NaOH, and demineralized water. The supporting equipment for the synthesis is a hotplate magnetic stirrer, measuring cup, reaction glass, filter paper, magnetic bar, and aluminum foil.

Preparation of green betel (*Piper betle* L.) leaf extract

The collected green betel leaves are cleaned with running water to remove dirt attached to the leaves and then dried in the sun for about seven days to reduce the water content in the leaves. The dried green betel leaves are cut into small pieces and mashed using a blender. In manufacturing, the dry green betel leaf extract is mixed with demineralized water with a ratio of 20:100 (g/mL). The heating process was carried out for 20 minutes at 80°C with a stirring speed of 700 rpm on a hot plate. Then the resulting extract was cooled at room temperature, and the extract obtained was filtered using filter paper. For this one extraction recipe, 40 mL of green betel leaf extract solution was obtained, and then it was ready to synthesize Fe_3O_4 nanoparticles.

Green synthesis of Fe_3O_4 nanoparticles

The process of synthesis of Fe_3O_4 nanoparticles in this study used the method reported by Altaf et al. (2021). Namely with the following steps: by mixing a

solution of chloride tetrahydrate ($FeCl_2.4H_2O$) and ferric chloride hexahydrate ($FeCl_3.6H_2O$) as precursors of Fe^{2+} and Fe^{3+} ions, with a mole ratio of 1:2 , then dissolved in 500 mL of distilled water with light stirring at 80°C; after complete dissolution a light orange color will be obtained, then 25 mL of green betel leaf extract (from the extraction result of ~40 mL for one recipe) is added while stirring over a magnetic stirrer; and the final result, the solution turns brownish black; then added 100 mL of 1 M NaOH until a black precipitate of magnetite (Fe_3O_4) was obtained.

Furthermore, after stirring for 5 minutes, the solution was taken from the stirrer and allowed to precipitate from the iron oxide nanoparticles precipitate. The black magnetite (Fe_3O_4) precipitate was washed five to eight times with distilled water. The washed residue was then dried in an oven at 80°C for 8 hours. The resulting magnetite particles were placed in a tightly closed medium for further characterization. The series of green synthesis methods are presented in Figure 1. Fe_3O_4 nanoparticles were obtained by adding base (NaOH) to a mixture of precursors (Fe^{2+} and Fe^{3+}) with a mole ratio of 1:2. The chemical reaction for the formation of Fe_3O_4 nanoparticles can be written as follows (Yew et al., 2016):

$$Piper\ betle\ L.\ \text{extract} + H_2O_{(l)} + Fe^{2+}_{(aq)} + Fe^{3+}_{(aq)} \xrightarrow{\text{Stirring}} [Piper\ betle\ L./Fe^{3+}\text{-}Fe^{2+}] \quad (1)$$

$$[Piper\ betle\ L./Fe^{3+}\text{-}Fe^{2+}] + 80H^-_{(aq)} \xrightarrow{\text{Stirring}} [Piper\ betle\ L./Fe_3O_4]\downarrow_{(s)} + 4H_2O_{(aq)} \quad (2)$$

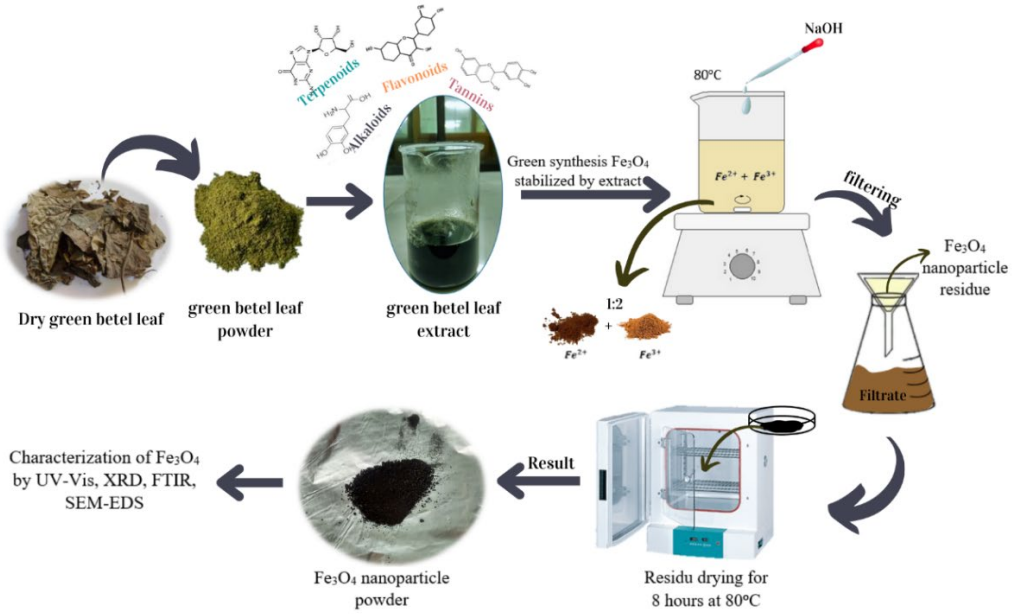

Figure 1. Schematic of the synthesis of Fe_3O_4 nanoparticles using the green synthesis method.

Characterization of Fe_3O_4 nanoparticles

UV-Visible Spectroscopy

UV-Visible spectroscopy was performed on green betel leaf extract and Fe_3O_4 nanoparticles. A total of 1 g of synthesized Fe_3O_4 nanoparticles were mixed with 20 mL of distilled water under mild stirring at room temperature for 15-20 minutes. Then a UV-Visible spectroscopy study was conducted with a wavelength range between 300 nm to 800 nm.

X-ray diffraction (XRD)

X-ray diffraction (XRD) was used to determine the crystalline phase of Fe_3O_4 nanoparticles. XRD patterns were recorded with an X-ray diffractometer using Cu-Kα radiation (λ= 1.5406 Å, 30 mA, 40 kV). The samples analyzed were in powder form. The parameters used for XRD analysis are: 2θ range = 20°- 65°, step size = 0.017°, and gap difference = 1°. The XRD data obtained were processed using Qual-X software and Origin Lab.

Fourier-transform infrared spectroscopy (FTIR)

FTIR was carried out to identify the functional groups of the nanoparticles produced with the addition of extract and without the addition of extract. The FTIR spectrum was measured with a scale range of 4000 cm^{-1} to 400 cm^{-1}.

SEM-EDS

Morphological analysis and chemical elements contained in the synthesized Fe_3O_4 nanoparticles were examined by Scanning Electron Microscopy (SEM) with HITACHI FLEXSEM 1,000 equipped with Energy Dispersive X-Ray Spectroscopy (EDS). The acceleration voltage of the microscope used is 8.00 kV, and the selected magnification is 2.000x and 10.000x.

HR-TEM

The High-Resolution Transmission Electron Microscope (HRTEM) is a tool for imaging the detailed internal structure of a sample in high resolution. Analysis of Fe_3O_4 particles was used by TEM H9500, which has a maximum acceleration voltage of 300kV. Among them can be used to analyze the shape and size of particles to the order of nanometers.

Vibrating Sample Magnetometer (VSM)

VSM250 was used to analyze the magnetic properties of the samples, which were visualized by hysteresis curves (M-H loop) and magnetic curves (M-H curve) at room temperature.

Adsorption studies

The magnetite nanoparticle adsorption test was carried out to determine the most effective adsorption ability based on the variation of the contact time used. A total of 0.5 g sample of magnetite nanoparticles was used to adsorb 50 mL of methylene blue solution with a concentration of 10 ppm with various contact times of 0, 30, 60, and 120 minutes. The process is carried out using a shaker according to the contact time used at room temperature. The concentration of un-adsorbed methylene blue was measured using a UV-Vis spectrophotometer in the wave length range of 400 nm to 800 nm.

RESULTS

UV-Visible spectroscopic analysis

Figure 2 shows the results of UV-Visible spectroscopy for green betel leaf extract and Fe_3O_4 nanoparticles. It can be seen that there is an absorption peak at 324 nm, which proves that the green betel leaf extract contains alkaloids, flavonoids, tannins, terpenoids, and carbohydrates (Heliawati, et.al, 2022; Madhumita, et.al, 2020). Meanwhile, Fe_3O_4 nanoparticles obtained continuous absorption from 300 nm to 800 nm. Figure 2b shows the band gap energy value of 1.87 eV.

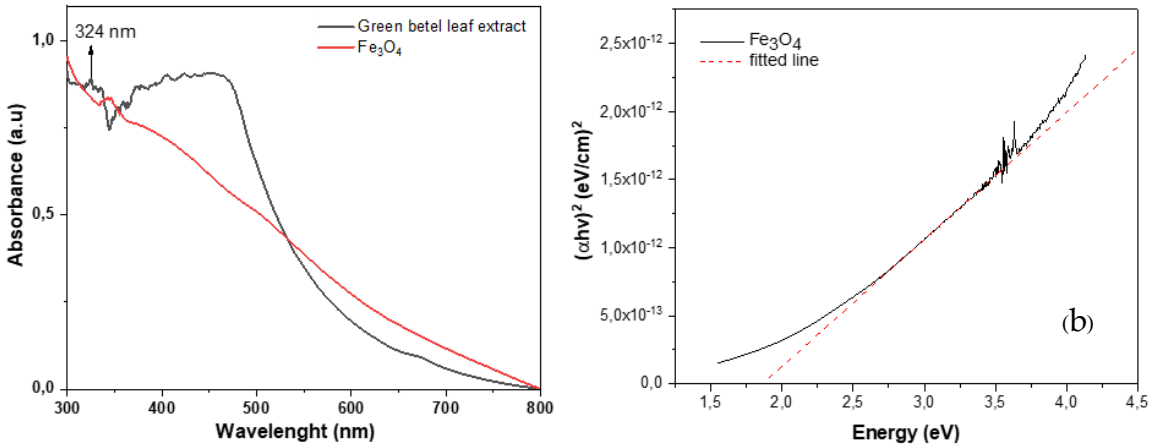

Figure 2. (a) UV-Vis absorption spectra of green betel extract and Fe_3O_4 nanoparticles (b) Band gap Fe_3O_4 nanoparticles.

XRD analysis

XRD pattern of Fe_3O_4 nanoparticles from green betel (*Piper betle* L.) leaf extract is presented in Figure 2a. It is seen that the diffraction peaks of the synthesized Fe_3O_4 nanoparticles are per previous studies; the identified crystal planes for Fe_3O_4 nanoparticles synthesized from iron sand natural materials are (220), (311), (400), (511), (440), at position 2θ = 30.3°, 35.5°, 43.2°, 57.0°, and 62.8° respectively. In the current preparation of magnetite nanoparticles (with green synthesis, using green betel extraction), there appears to be one more crystal field peak at (422). The data is well confirmed in the JCPDS database No. 19-0629, as the magnetite (Fe_3O_4) phase.

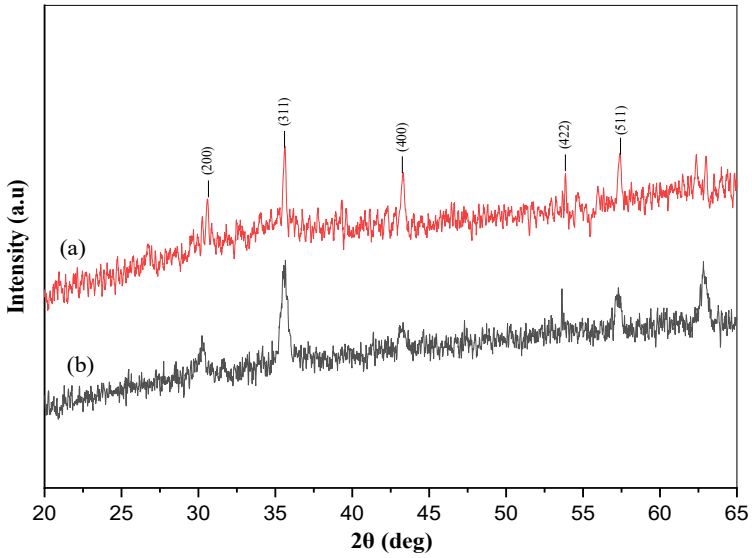

Figure 3. XRD pattern (a) Synthesis of Fe_3O_4 from green betel leaf extract (b) Fe_3O_4 from previous studies (Munasir & Terraningtyas, 2019).

FTIR analysis

FTIR characterization was carried out to determine the functional groups in the synthesized samples that have a role in forming Fe_3O_4 nanoparticles. The FTIR spectrum curves for green betel leaf extract and Fe_3O_4 nanoparticles are shown in Figure 4. The FTIR spectrum of the synthesis results shows that there are absorption bands at 482 cm^{-1} and 567 cm^{-1}, which indicate the presence of Fe-O functional groups.

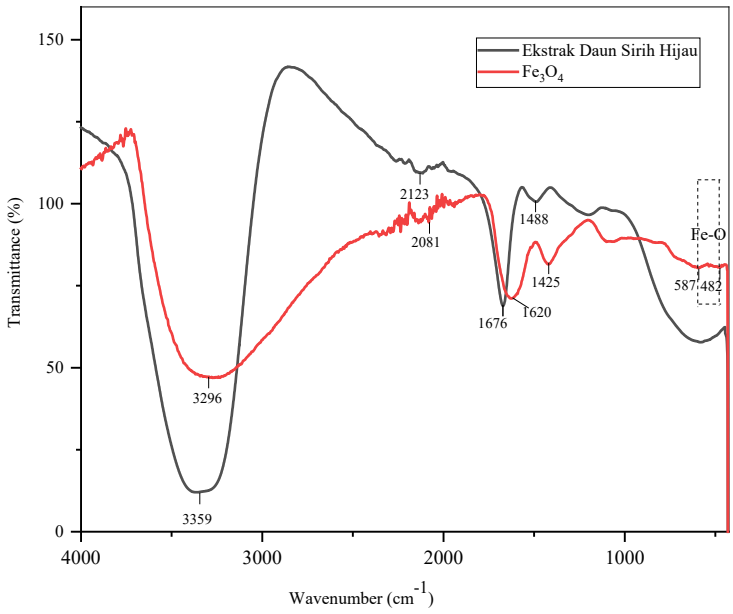

Figure 4. FTIR spectrum of Fe_3O_4 (synthesized: green betel leaf extract).

Morphology analysis

SEM images show that the particles agglomerate, so the resulting morphology is irregular with a coarse grain structure (Figure 5a). After magnification with a scale of 5 µm, the particles produced were needle-shaped (Figure 5b).

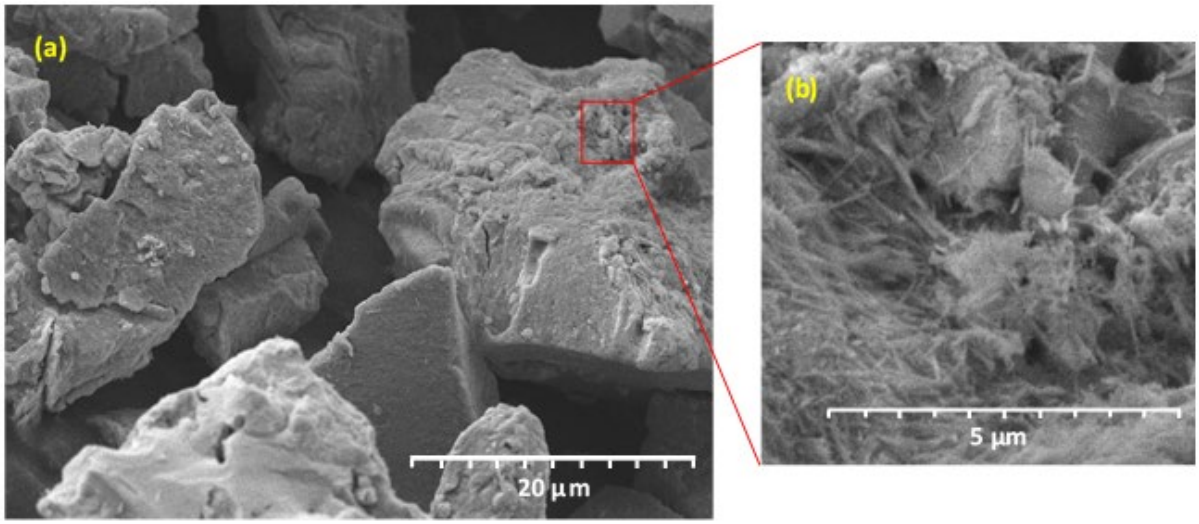

Figure 5. (a) Morphology of Fe_3O_4 nanoparticles (b) Morphological magnification at 5 µm (synthesized: green betel leaf extract).

Figure 6 shows the Fe_3O_4 particles morphology. The magnetic Fe_3O_4 particles have nanometer size, spherical or spherical shape, homogeneous and regular morphology, and a typical spinel crystal structure (supported by XRD data). All these characteristics are significant for the magnetic applications of Fe_3O_4. Spinel Fe_3O_4 comprises metal and oxygen ions arranged in a series of regular crystals; the iron ion (Fe) has two oxidation states, namely Fe^{2+} and Fe^{3+}, and eight oxygen ions (O). This spinel structure supports the good magnetic of Fe_3O_4. TEM images clearly show that Fe_3O_4 nanoparticles are spherical and needle shapes (Figure 6(a-b)) and these particles agglomerate due to the hydroxyl form of green betel leaf extract. The average particle size of the synthesized Fe_3O_4 nanoparticles measured by the image J software was 29.82 nm (Figure 6(c-d)).

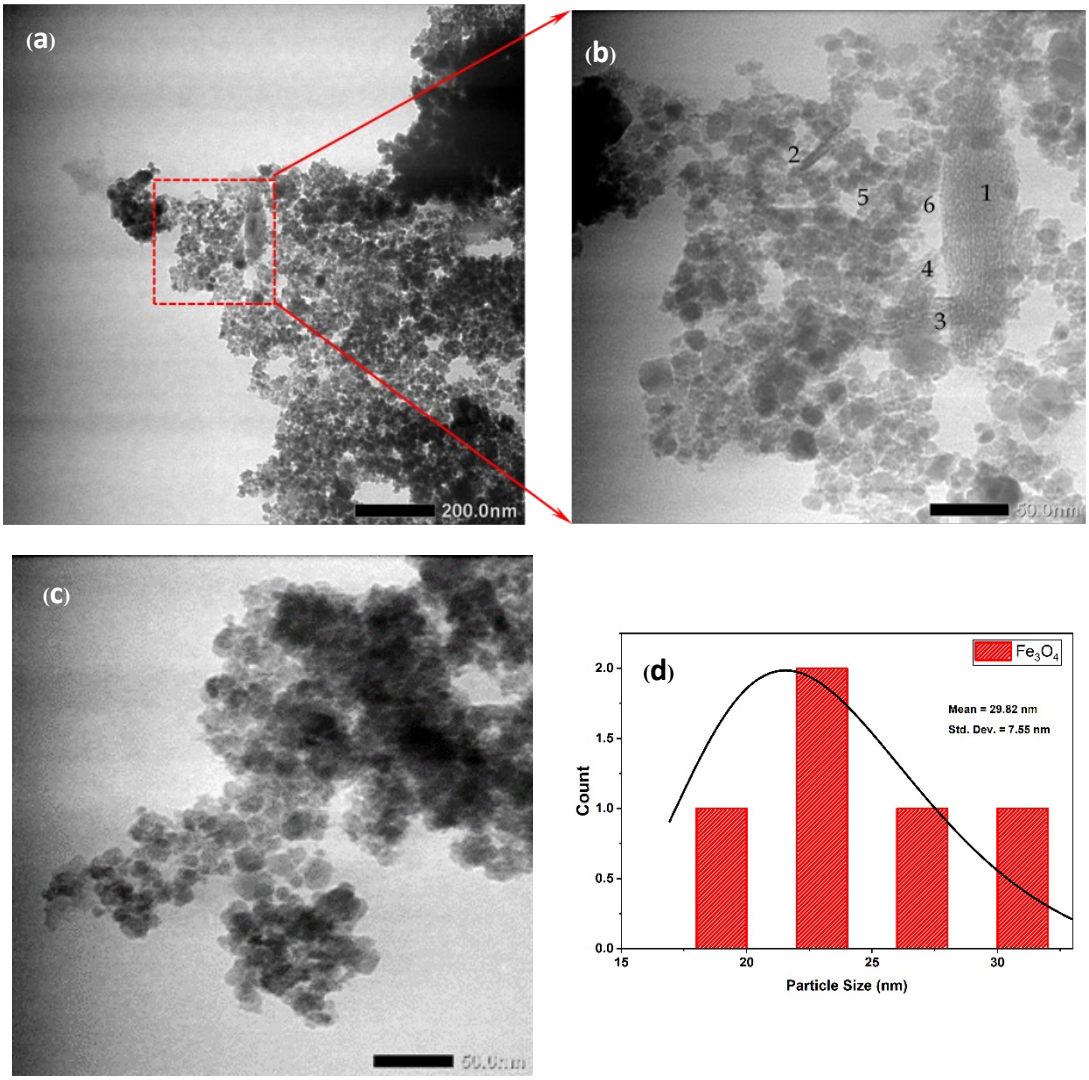

Figure 6. HR-TEM morphology: (a-b) spherical and needle-like particles, (c) spherical particles, and (d) histogram of estimated size of Fe_3O_4 nanoparticles that have been synthesized using green betel leaf extract.

EDS analysis

EDS characterization was carried out to determine the composition of the synthesized sample's chemical elements, as shown in Figure 7. It can be seen that the peak amplitude of iron is around 6.5 keV, which indicates the presence of iron elements as well as a high percentage of iron in the particles using EDS.

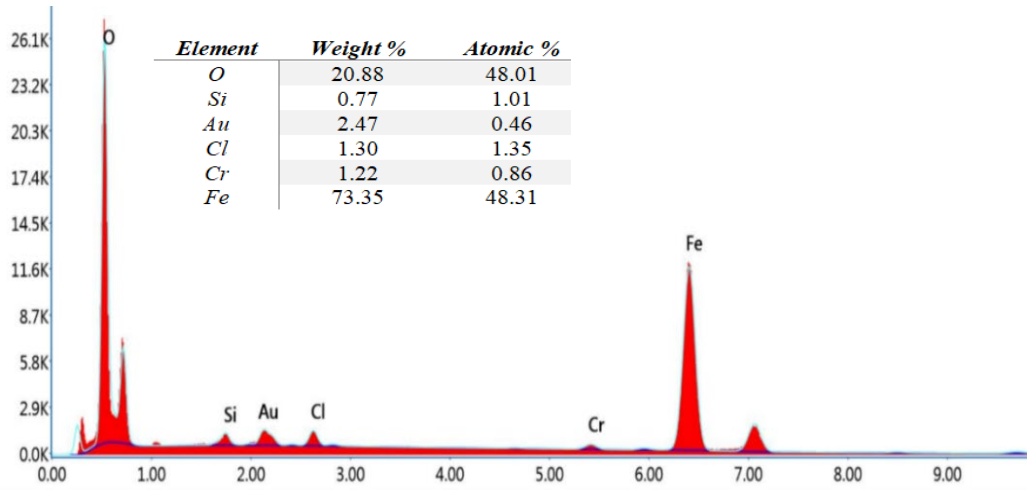

Figure 7. EDS results from Fe_3O_4 nanoparticles (synthesized: green betel leaf extract).

VSM Analysis

The VSM characterization was used to determine the magnetic properties of the synthesized results in the form of a magnetization curve as shown in Figure 8. The magnetization curve shows ferromagnetic behavior with a saturation magnetization (Ms) value of 9.18 emu/g, remanent magnetization (Mr) 0.49 emu/g, and a coercive field (Hc) 78.22 Oe.

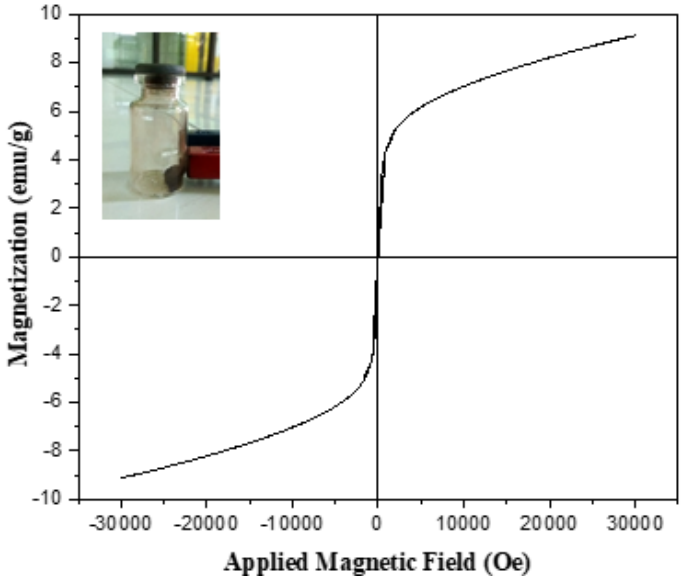

Figure 8. Room temperature magnetization curve of Fe_3O_4 nanoparticles from green betel (*Piper betle* L.) leaf extract.

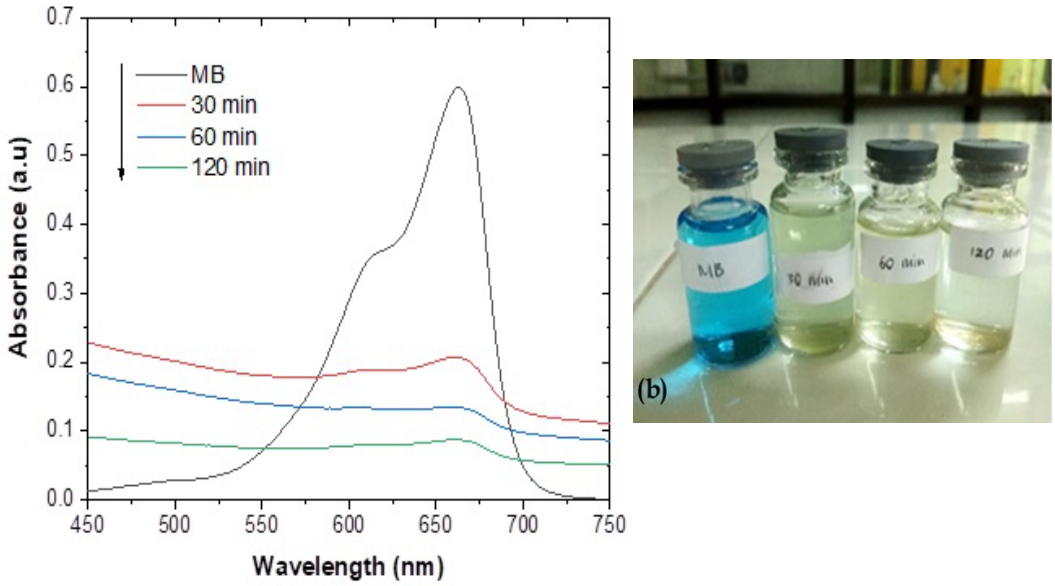

Figure 9. (a) Absorption spectrum of UV-Vis adsorbed by time variation of Fe_3O_4 nanoparticles (b) result of time variation of adsorption filtrate.

Adsorption Analysis

Figure 9a shows the results of UV-Vis absorption from methylene blue solution that has been adsorbed by Fe_3O_4 nanoparticles, it can be seen that there is a decrease in intensity with the length of contact time. The significant color change in methylene blue when adsorbed by magnetite is shown in Figure 9b. The removal adsorption percentages of Fe3O4 nanoparticles for methylene blue with a time of 30, 60, and 120 minutes were found to be 87.20%, 93.39%, and 98.75%, respectively.

DISCUSSION

The UV-Visible spectroscopy of green betel (*Piper betle* L.) and Fe_3O_4 nanoparticles is shown in Figure 2a. Green betel (*Piper betle* L.) leaf extract has an absorption band of 324 nm, which is associated with alkaloids, flavonoids, tannins, terpenoids, and carbohydrates in green betel extract. The phytochemicals in green betel leaf extract are bound to the surface of the nanoparticles rich in hydroxyl and hydrophilic groups, thus enabling the nanoparticles to disperse and distribute homogeneously in an aqueous solution. The synthesized Fe_3O_4 nanoparticles showed continuous absorption in the visible range between 300 nm to 800 nm due to the absorption and electronic transitions by Fe_3O_4 nanoparticles (Yew et al., 2016).

An electronic transition in a molecule occurs when an electron in one of the molecular orbitals is excited to a higher energy orbital; when a molecule absorbs electromagnetic light, such as UV-Vis light, the electrons in the molecule transition to a higher energy orbital. After that, the absorbed beam will have an energy equal to the energy difference between the initial and final orbitals, according to the Beer-Lambert law. In Fe_3O_4, there is a transition from electrons in d orbitals on Fe^{2+} ions to d orbitals on Fe^{3+} ions. This transition can occur in the UV-Vis range; Fe_3O_4 molecules can absorb UV-Vis light at specific wavelengths (Safitri, et al., 2021). In the wavelength range of 300-800 nm, electrons in molecules or atoms usually undergo electronic transitions from σ orbitals to σ* orbitals or from σ orbitals to π* orbitals, which require energies of about 1.6 to 3.3 eV. However, the adsorption mechanism that occurs in visible light with a wavelength range of 300-800 nm depends on the nature of the material and the surrounding

environment, so it needs to be explicitly analyzed in some instances (El Ghandoor et al., 2012). The size of the band-gap of Fe_3O_4 and other materials is strongly influenced by the nature of the material and the environment for the synthesis process (Saragi et al., 2018; Strehlow and Cook).

The peak of the leaf extract in the spectrum of Fe_3O_4 nanoparticles indicates the presence of alkaloids, flavonoids, tannins, terpenoids, and carbohydrates. Phytochemicals act as reducing agents and capping agents for synthesizing Fe_3O_4 nanoparticles. The energy gap of the synthesized sample is calculated based on UV-Vis data using the Tauc equation as follows (Tauc et al., 1966):

$$(\alpha hv)^2 = B\left(hv - E_g\right) \quad (3)$$

where *a* is the adsorption coefficient, *B* is a constant, *h* is Planck's constant, *v* is the photon frequency and E_g is the energy gap. Based on the calculation using tauc-plot, the band-gap value of Fe_3O_4 nanoparticles is 1.87 eV (Figure 2b) which indicates that Fe_3O_4 material is classified as a semiconductor material.

X-ray diffraction (XRD) is an effective characterization to confirm the crystal structure of the synthesized Fe_3O_4 nanoparticles. The XRD pattern obtained for Fe_3O_4 nanoparticles synthesized using green betel (*Piper betle* L.) leaf extract is shown in Figure 3a. The diffraction peaks of the synthesized Fe_3O_4 nanoparticles were detected at angles of 2θ = 20.58°, 35.6°, 53.86° and 57.38° with the crystal planes of (200), (300), (400), (422), and (511). The diffraction peaks were analyzed and matched with the previous study's XRD pattern, shown in Figure 3b (Munasir et al., 2020, 2022; Munasir and Terraningtyas, 2019). The estimated mean crystal size of Fe_3O_4 nanoparticles can be calculated using the Debye-Scherrer equation, which provides a relationship between peak broadening in XRD and crystal size. The Debye-Scherrer equation is shown as follows:

$$d = \frac{k\lambda}{\beta_{hkl} cos\theta_{hkl}} \quad (4)$$

where *d* is the crystal size of the synthesized Fe_3O_4 nanoparticles for the phase (*hkl*), *k* is the Scherrer constant (0.9), is the wavelength of X-ray radiation for Cu Kα (1.15406), β_{hkl} is the value of full-width at half maximum (FWHM) at the peak (*hkl*) in radians, and θ_*hkl* is the Bragg diffraction angle for the phase (*hkl*). According to the calculation using the Scherrer equation, the average crystal size of the synthesized magnetic nanoparticles was 6.93 nm.

FTIR analysis was used to characterize the synthesized Fe_3O_4 nanoparticles, understand the presence of functional groups in green betel leaf extract, and predict their role in synthesizing Fe_3O_4 nanoparticles. Figure 4 shows the FTIR spectrum curve of green betel leaf extract and Fe_3O_4 nanoparticles. Both curves show that there are variations in peak intensity in different areas. The spectrum of green betel leaf extract showed strong absorption bands at 3,359 cm^{-1}, 2,123 cm^{-1}, 1,676 cm^{-1}, and 1,488 cm^{-1}, while the absorption bands of the synthesized Fe_3O_4 nanoparticles were at 3,296 cm^{-1}, 2,081 cm^{-1}, 1,620 cm^{-1}, 1,425 cm^{-1}, 587 cm^{-1}, and 482 cm^{-1}. The absorption peak of 3,359 cm-1 in green betel leaf extract indicated the presence of O-H strain vibrations which proved the presence of polyphenol groups (Priya et al., 2014). This peak shifted from 3,359 cm^{-1} to 3,296 cm^{-1}, indicating that the O-H phenol group acted as a reducing agent in forming Fe_3O_4 nanoparticles. The absorption peak shifted from 2,123 cm^{-1} to 2,081 cm^{-1}, contributing to the C-H strain vibration of the $-CH_2$ functional group. The shift in the absorption band from 1,676 cm^{-1} to 1,620 cm^{-1} was associated with binding the C=O group of carboxylic acids to the nanoparticles (Kannan et al., 2013). At the same time, the shift in the absorption band from 1,488 cm^{-1} to 1,425 cm^{-1} indicates the presence of C=C groups of aromatic compounds and amide groups. The formation of Fe_3O_4 nanoparticles was characterized by two absorption bands at 567 cm^{-1} and 482 cm^{-1} in the spectrum of the synthesized Fe_3O_4 nanoparticles related to the Fe-O strain vibration mode. The metal-oxide band at 567 cm^{-1}

corresponds to the intrinsic strain vibration of the metal at the tetrahedral site, while the metal-oxide band found at 482 cm^{-1} indicates the octahedral-metal Fe-O strain (Demir et al., 2013). The formation of Fe_3O_4 nanoparticles was confirmed by characteristic peaks located in the region between 400 cm^{-1} and 600 cm^{-1} corresponding to Fe_3O_4 (Yuvakkumar & Hong, 2014).

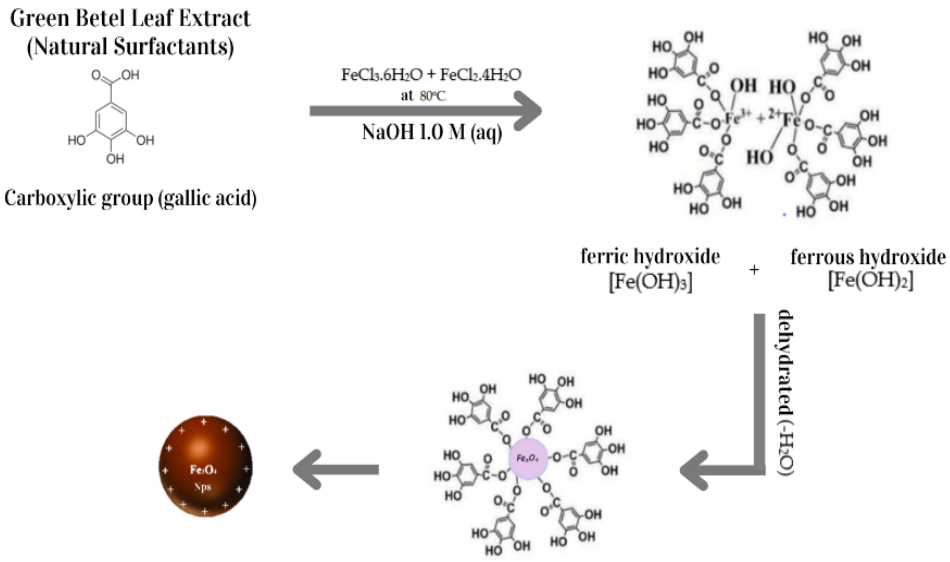

Figure 10. The mechanism of formation of Fe_3O_4 nanoparticles uses a green betel leaf extraction solution.

A possible mechanism for forming Fe_3O_4 nanoparticles using green betel (*Piper betle* L.) leaf extract is shown in Figure 10. The reaction mixture consisted of green betel leaf extract, ferrous chloride tetrahydrate ($FeCl_2.4H_2O$), and ferric chloride hexahydrate ($FeCl_3.6H_2O$). Based on the results of FTIR (Figure 4) supports the presence of a C=O carboxylate group in the green betel leaf extract, namely at a wave number of 1,676 cm^{-1}. Furthermore, the illustration of the mechanism of interaction between the precursors ($FeCl_2$ and $FeCl_3$) with chemical compounds contained in green betel leaf extract (gallic acid) is shown in the reaction mechanism in Figure 10. Based on the mechanism of forming Fe_3O_4 nanoparticles (Figure 10), it is known that gallic acid is a phytochemical contained in green betel (*Piper betle* L.) leaf extract. The carboxylic group (gallic acid) of green betel leaf extract forms a complex with Fe^{3+} and Fe^{2+}. Because the reaction was carried out at a temperature of 80°C, the OH- of NaOH took part in the reaction, so there would be rivalry between the $COO^-...Fe^{3+}$ and $COO^-...Fe^{2+}$ bonds and the formation of $HO^-...Fe^{3+}$ and $OH^-...Fe^{2+}$ bonds, therefore the formation of ferric hydroxide [$Fe(OH)_3$] and ferrous hydroxide [$Fe(OH)_2$]. The reaction mixture of ferric hydroxide and ferrous hydroxide will form dehydration (^-H_2O) to produce Fe_3O_4 nanoparticles (Ramesh et al., 2018).

Scanning electron microscopy (SEM) was used to analyze the structure of the nanoparticles. Figure 5a shows the SEM results of Fe_3O_4 nanoparticles with a scale of 20 µm. It can be seen that the particles formed are not the same. The morphology distribution is irregular, and the particles are shaped like plates with a coarse grain structure. This undetectable form was detected due to the agglomeration process, which is probably related to the interparticle forces, strong Van der Waals forces, high surface area to volume ratio, and magnetic attraction between nanoparticles (Yusefi et al., 2021). According to Rahimah et al. (2019), the agglomeration caused in the synthesis is very difficult to avoid. This is due to the magnetic properties of the nanomagnets, which cause an attractive force between particles so that clumping or agglomeration will occur. Figure 5b is a

morphological enlargement of Figure 5a with a scale of 5 µm. After magnification, it is seen that the particles obtained are shaped like needles, have been reported by Khaira et al. (2020). The size and particle size of Fe_3O_4 are highly dependent on the composition of the addition of precursor (Fe^{2+} and Fe^{3+}) and the type of salt used, which in this study used a mole ratio of iron salt, which is 1:2 ($FeCl_2$: $FeCl_3$). In addition, the type of extract used in the synthesis also affects the morphology of the resulting nanoparticles.

Table 1. Examples of Fe_3O_4NPs prepared using the Green Synthesis method.

Plant Extract	*Chemical Composition*	Size		References
		Particles	*Crystalline*	
Red betel leaf (Piper crocatum)	flavonoids, alkaloids, terpenoids, cyanogenic, glucoside, isoprenoid, nonprotein amino acid and eugenol	≈ 30 nm Needle-shaped	≈26.66 nm	(Khaira, Ulianas, et al., 2020)
Rambutan fruit (Nephelium lappaceum L), from Thailand	sucrose, fructose glucose and organic acid (citric acid, tartaric, malic, succinic and lactic acids)	≈ 100-200 nm, spinel shape	-	(Yuvakkumar & Hong, 2014)
Leaf extract of Platanus orientalis	polyphenols, flavonoids, quercetin, kaempferol, glycosides, and tannins	≈38 nm, spherical shape	≈12.3 nm	(Devi et al., 2019)
Leaf extract of Zanthoxylum armatum DC	alkaloids, flavonoids, terpenoids, phenols, and steroids	≈17 nm, spherical shape	≈6 nm	(Ramesh et al., 2018) (Basavegowda et al., 2014)
Leaves extract of Artemisia Annua L.	saponins, glycosides, flavanoids, protein, triterpenoids	≈40-60 nm, cubical shape	19-24 nm	(Bouafia et al., 2021)
the extract of Citrus aurantium (CA)	flavonoids, coumarins, and terpenoids	≈5-50 nm Spherical shape	≈12.5 nm	(Bassim et al., 2022)
Azadirachta indica aqueous leaf extract	alkaloids, flavonoids, saponins, glycosides, phenols, steroids, tannins, reducing sugars and anthraquinones	≈11 nm, spherical	≈9-14 nm	(Taib et al., 2018)

Moreover, SEM and HR-TEM analysis results are consistent, especially in identifying needle-like particles(Khaira et al., 2020; Zhou et al., 2001). The shape and size of the particles are strongly influenced by the type of salt used, the ratio of Fe^{2+}/Fe^{3+}, and the type of extraction of organic compounds used. Green betel leaf extract acts as a capping agent to form particles such as needles, spheres, and spinels (Table 1).

Energy-dispersive X-ray spectroscopy (EDS) analysis was used to identify the composition and stoichiometry of the chemical elements of the synthesized iron oxide nanoparticles, as presented in Figure 7. X-rays reflect iron compounds to produce peak amplitudes that are useful for helping determine the elemental content present in the compound and the mixture of compounds in the sample. Elements of iron, oxygen, and other elements have also been detected. The peak amplitude of iron is about 6.5 keV, as in Figure 6, which indicates the presence of elemental iron (Fe) in the compound using EDS, which results indicate a high percentage of elemental iron in the particles. The Cl element probably came from the precursors ($FeCl_2$ and $FeCl_3$) used for the synthesis, while the peak appearance of the Si, Cr and Au elements was due to the presence of active polyphenol groups on the surface, according to the results of the FTIR spectrum. Another factor showed that the phytoconstituents of the green betel leaf extract limited the Fe_3O_4 nanoparticles, implying that overall the nanoparticles consisted of Fe and O with a mass content of 73.35% and 20.88%, respectively, as shown in Figure 7 (Kiwumulo et al., 2022; Lee et al., 2016; Ramesh et al., 2018).

Analysis of magnetic properties was carried out using a VSM tool. The information obtained is in the form of the magnitude of the magnetic properties due to changes in the external magnetic field which is described by a hysteresis curve. The magnetization curve of the synthesized Fe_3O_4 nanoparticles is presented in Figure 7. The magnetization curve shows ferromagnetic behavior with

a saturation magnetization value (Ms) of 9.18 emu/g, a remanent magnetization (Mr) of 0.49 emu/g, and a coercive field (Hc) of 78.22 Oe. Similar experimental results were also obtained from Venkateswarlu et al. (2014) who reported the ferromagnetic behavior of Fe_3O_4 nanoparticles with magnetization, Ms=13.6 emu/g. The top-left insert in Figure 8 shows the behavior of magnetic nanoparticles when subjected to an external magnetic field. The saturation value can be influenced by several factors such as particle size, degree of crystallinity and the presence of an impurity phase.

The adsorption test on methylene blue was carried out by studying the effect of contact time variations. Adsorption was carried out by mixing 0.5 g of synthesized magnetite into 50 mL of methylene blue solution with a concentration of 10 ppm at contact times of 0, 30, 60, and 120 minutes. The UV-Vis absorption spectrum of methylene blue which is not adsorbed in solution at time "t" after being adsorbed by Fe_3O_4 nanoparticles is shown in Figure 9a. The significant color change in methylene blue when adsorbed by magnetite is shown in Figure 9b. Based on Figure 9a, it can be observed that the adsorption ability of the synthesized magnetite decreased with increasing time. The results of the decrease in the absorbance value can be used to determine the percentage adsorption of solution color or dyes removal efficiency (or $\%RE_{MB}$) using the following equation:

$$\%RE_{MB} = \left(1 - \frac{C_t}{C_o}\right) \times 100\% \quad (5)$$

$$Adsorption\ Capacity\left(\frac{mg}{g}\right) = \frac{(C_0 - C_t)V}{m} \quad (6)$$

C_0 and C_t respectively represent the initial concentration and concentration of the MB solution after t the adsorption process, m is the mass of the absorbent (Fe_3O_4 NPs powder), and V represents the volume of the MB solution (Munasir et al., 2020). Based on equations 5 and 6, the graph between the adsorption capacity and the percent removal of MB is shown in Figure 11. The adsorption capacities obtained at various contact times of 30, 60, and 120 minutes were 0.872, 0.934, and 0.987 mg/g, with the removal percentages 87.20, 93.39, and 98.75%, respectively.

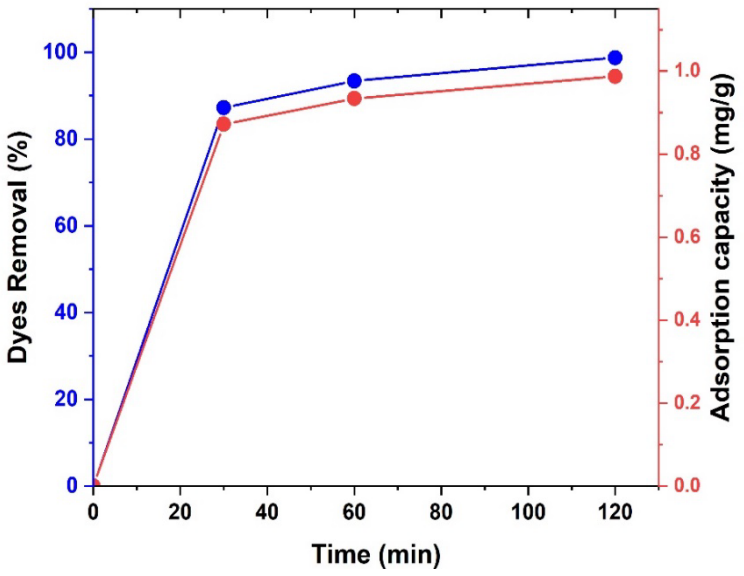

Figure 11. Removal efficiency of methylene blue in the water and adsorption capacity (mg/g)

The longer the contact time between the adsorbent (magnetite) and the adsorbate (MB), the more adsorbate will be adsorbed and the adsorption will increase. In accordance with the concept, that the longer the adsorption time required between the adsorbent and the solute, the more substances will be adsorbed but the amount of solute adsorbed will reach a limit value at a certain time where the adsorbent is no longer able to absorb the solute due to saturation on the surface of the adsorbent. At the time of stirring for 120 minutes the concentration of the adsorbed methylene blue dye decreased because the bond of the methylene blue dye group became weaker and finally released back into the solution. So that only groups that are strongly bound to the adsorbent can still bind or this is called the desorption process. In addition, because of the influential stirring factor and the shaker factor that is too fast or the rpm is too fast. Where initially bound, becomes unbound then bonded again and then released again because the weak bond causes methylene blue to experience a change in charge. In this case, the bond that occurs is not a very strong chemical bond but only based on electrostatic forces.

CONCLUSION

Based on the research results, the synthesis of Fe_3O_4 nanoparticles from green betel leaves (*Piper battle* L.) using the green synthesis method, the resulting particles cannot be claimed to be nano-sized. UV-Vis spectroscopy investigated the formation of Fe_3O_4, which exhibits continuous absorption at wavelengths between 300 nm and 800 nm. The band gap energy of magnetite is 1.87 eV, and it is classified as a semiconductor material. XRD analysis confirmed a crystal size of 6.93 nm Fe_3O_4. FTIR results indicate the presence of functional groups from leaf extracts that play a role in forming Fe_3O_4. SEM results were obtained as needle-like particles (confirmed by HR-TEM data). The HR-TEM images show nano-sized, mainly spherical, and needle-like particles with an average particle size of 29.82 nm. The percentage of Fe and O elements shows the dominant content of iron oxide Fe_3O_4, with a mass content of 73.35% and 20.88%. The magnetization curve shows that the synthesized green magnetite has ferromagnetic properties. The ferromagnetic properties of Fe_3O_4 were then applied as an efficient adsorbent to remove methylene blue and observed using UV-Vis spectroscopy; the most effective absorption ability was at a contact time of 120 minutes with an adsorption capacity of 0.987 mg/g, and the percentage of MB degradation was 98.75%.

ACKNOWLEDGMENTS

The author would like to thank the Materials Laboratory of the Physics Department, Universitas Negeri Surabaya (Unesa), the Laboratory of Chemistry, State University of Surabaya, the Laboratory of Materials and Metallurgy of the Institut Teknologi Sepuluh Nopember Surabaya (ITS), and the Integrated Laboratory of the Universitas Negeri Malang (UM) for providing facilities and conveniences in research activities and sample testing.

REFERENCES

Agnestisia, R. 2017. Synthesis & characterization of magnetit (Fe_3O_4) and its applications as adsorbent methylene blue. Jurnal Sains Dan Terapan Kimia. 11(2): 61-70.

Aksu Demirezen, D., Yıldız, Y. Ş., Yılmaz, Ş., and Demirezen Yılmaz, D. 2019. Green synthesis and characterization of iron oxide nanoparticles using *Ficus carica* (common fig) dried fruit extract. Journal of Bioscience and Bioengineering. 127(2): 241–245.

Altaf, S., Zafar, R., Zaman, W. Q., Ahmad, S., Yaqoob, K., Syed, A., Khan, A. J., Bilal, M., and Arshad, M. 2021. Removal of levofloxacin from aqueous solution by green synthesized magnetite (Fe_3O_4) nanoparticles using *Moringa olifera*: Kinetics and reaction mechanism analysis. Ecotoxicology and Environmental Safety. 226: 112826.

Bagbi, Y., Sarswat, A., Mohan, D., Pandey, A., and Solanki, P. R. 2016. Lead (Pb^{2+}) adsorption by monodispersed magnetite nanoparticles: Surface analysis and effects of solution chemistry. Journal of Environmental Chemical Engineering. 4(4): 4237–4247.

Bassim, S., Mageed, A. K., AbdulRazak, A. A., and Majdi, H. Sh. 2022. Green synthesis of Fe_3O_4 nanoparticles and its applications in wastewater treatment. Inorganics. 10(12): 260.

Basavegowda, N., Somai Magar, K. B., Mishra, K., and Lee, Y. R. 2014. Green fabrication of ferromagnetic Fe_3O_4 nanoparticles and their novel catalytic applications for the synthesis of biologically interesting benzoxazinone and benzthioxazinone derivatives. New Journal of Chemistry, 38(11): 5415–5420.

Bouafia, A., Laouini, S. E., Khelef, A., Tedjani, M. L., & Guemari, F. (2021). Effect of ferric chloride concentration on the type of magnetite (Fe_3O_4) nanoparticles biosynthesized by aqueous leaves extract of artemisia and assessment of their antioxidant activities. Journal of Cluster Science. 32(4): 1033–1041.

Chomchoey, N., Bhongsuwan, D., and Bhongsuwan, T. 2018. Effect of calcination temperature on the magneticcharacteristics of synthetic iron oxide magneticnanoparticles for arsenic adsorption. Chiang Mai Journal of Sciences. 45(1): 528–539.

Dalimartha, S. (2006). Atlas of Indonesian medicinal plants: Revealing the wealth of Indonesian medicinal plants (Cet. 7). Trubus Agriwidya. Jakarta

Demir, A., Topkaya, R., and Baykal, A. 2013. Green synthesis of superparamagnetic Fe_3O_4 nanoparticles with maltose: Its magnetic investigation. Polyhedron. 65: 282–287.

Devi, H. S., Boda, M. A., Shah, M. A., Parveen, S., and Wani, A. H. 2019. Green synthesis of iron oxide nanoparticles using *Platanus orientalis* leaf extract for antifungal activity. Green Processing and Synthesis, 8(1): 38–45.

El Ghandoor, H., Zidan, H. M., Mostafa M.H., Khalil and Ismail, M. I. M. 2012. Synthesis and some physical properties of magnetite (Fe_3O_4) nanoparticles. International Journal of Electrochemical Science. 7: 5734 – 5745.

Ghaedi, M., Hajjati, S., Mahmudi, Z., Tyagi, I., Agarwal, S., Maity, A., and Gupta, V. K. 2015. Modeling of competitive ultrasonic assisted removal of the dyes – Methylene blue and Safranin-O using Fe3O4 nanoparticles. Chemical Engineering Journal. 268: 28–37.

Heliawati, L., Lestari, S., Hasanah, U., Ajiati, D., and Kurnia, D. 2022. Phytochemical profile of antibacterial agents from red betel leaf (*Piper crocatum* Ruiz and Pav) against bacteria in dental caries. Molecule. 27(9): 1-19.

Iconaru, S. L., Guégan, R., Popa, C. L., Motelica-Heino, M., Ciobanu, C. S., and Predoi, D. 2016. Magnetite (Fe_3O_4) nanoparticles as adsorbents for as and Cu removal. Applied Clay Science. 134: 128–135.

Kannan, R. R. R., Stirk, W. A., and Van Staden, J. 2013. Synthesis of silver nanoparticles using the seaweed *Codium capitatum* P.C. Silva (Chlorophyceae). South African Journal of Botany. 86: 1–4.

Khaira, R., Ulinas, A., and Azhar, M., 2020. Synthesis of magnetic iron oxide (Fe_3O_4) nanoparticles using red betel leaf extract (*Piper crocatum*) as a capping agent. Periodic. 9(2): 42–46.

Kiwumulo, H. F., Muwonge, H., Ibingira, C., Lubwama, M., Kirabira, J. B., and Ssekitoleko, R. T. 2022. Green synthesis and characterization of iron-oxide nanoparticles using *Moringa oleifera*: A potential protocol for use in low and middle income countries. BMC Research Notes, 15(1), 1–8.

Latha, N., and Gowri, M. 2014. Biosynthesis and characterisation of Fe_3O_4 nanoparticles using *Caricaya* papaya leaves extract. International Journal of Science and Research. 3(11): 1551–1556.

Lee, K. L., Shameli, K., Miyake, M., Kuwano, N., Bahiyah, N., Eva, S., and Yew, Y. P. 2016. Green synthesis of gold nanoparticles using aqueous extract of *Garcinia mangostana* fruit peels. Journal of Nanomaterials. 2016(2): 1-7.

Liu, X., Tian, J., Li, Y., Sun, N., Mi, S., Xie, Y., and Chen, Z. 2019. Enhanced dyes adsorption from wastewater via Fe3O4 nanoparticles functionalized activated carbon. Journal of Hazardous Materials. 373: 397-407.

Magdy, A., Fouad, Y. O., Abdel-Aziz, M. H., and Konsowa, A. H. 2017. Synthesis and characterization of Fe3O4/kaolin magnetic nanocomposite and its application in wastewater treatment. Journal of Industrial and Engineering Chemistry. 56: 299-311.

Mahdavi, M., Namvar, F., Ahmad, M. Bin, and Mohamad, R. 2013. Green biosynthesis and characterization of magnetic iron oxide (Fe_3O_4) nanoparticles using seaweed (*Sargassum muticum*) aqueous extract. Molecules. 18(5): 5954–5964.

Mahdavian, A. R. and Mirrahimi, M. A. S. 2010. Efficient separation of heavy metal cations by anchoring polyacrylic acid on superparamagnetic magnetite nanoparticles through surface modification. Chemical Engineering Journal. 159(1–3): 264–271.

Marciello, M., Connord, V., Veintemillas-Verdaguer, S., Vergés, M. A., Carrey, J., Respaud, M., Serna, C. J., and Morales, M. P. 2013. Large scale production of biocompatible magnetite nanocrystals with high saturation magnetization values through green aqueous synthesis. Journal of Materials Chemistry B. 1(43): 5995–6004.

Madhumita, M., Guha, P., Nag, A. (2020). Bio-actives of betel leaf (Piper betle L.): A comprehensive review on extraction, isolation, characterization, and biological activity, Phytotherapy Research. 34(10): 2609-2627.

Munasir and Terraningtyas, A. 2019. Synthesis and characterization of Fe_3O_4/SiO_2 composite with in-situ method: TEOS as SiO_2 NPs precursor. Journal of Physics: Conference Series. 1171(1): 6–11.

Munasir, Taufiq, A., Teraningtyas, A., Kusumawati, D. H., and Supardi, Z. A. I. 2022. Nanosized Fe_3O_4/SiO_2 core-shells fabricated from natural sands, magnetic properties, and their application for dye adsorption. Engineering and Applied Science Research. 49(3): 340–352.

Munasir, N., Kusumawati, R.P., Kusumawati, D. H., Supardi, Z. A. I., Ahmad, T, and Darminto. 2020. Characterization of Fe_3O_4/rGO composites from Natural Sources: Application for dyes color degradation in aqueous solution. International Journal of Engineering, Transactions A: Basics. 33(1): 18-27.

Padmavathy, K. S., Madhu, G., and Haseena, P. V. 2016. A study on effects of pH, adsorbent dosage, time, initial concentration and adsorption isotherm study for the removal of hexavalent chromium (Cr (VI)) from wastewater by magnetite nanoparticles. Procedia Technology. 24: 585–594.

Patil, S. B., Basavarajappa, P. S., Ganganagappa, N., Jyothi, M. S., Raghu, A. V., and Reddy, K. R. 2019. Recent advances in non-metals-doped TiO_2 nanostructured photocatalysts for visible-light driven hydrogen production, CO_2 reduction and air purification. International Journal of Hydrogen Energy. 44(26): 13022–13039.

Priya, B., Gupta, V. K., Pathania, D., and Singha, A. S. 2014. Synthesis, characterization and antibacterial activity of biodegradable starch/PVA composite films reinforced with cellulosic fibre. Carbohydrate Polymers. 109: 171–179.

Rahimah, R., Fadli, A., Yelmida, Y., Nurfajriani, N., and Zakwan, Z. 2019. Synthesis and Characterization Nanomagnetite by Coprecipitation. Indonesian Journal of Chemical Science and Technology. 2(2): 90-96.

Ramesh, A. V., Rama Devi, D., Mohan Botsa, S., and Basavaiah, K. 2018. Facile green synthesis of Fe_3O_4 nanoparticles using aqueous leaf extract of *Zanthoxylum* armatum DC. for efficient adsorption of methylene blue. Journal of Asian Ceramic Societies. 6(2): 145–155.

Rukmini, A., Utomo, D. H., and Laily, A. N. 2020. Skrining fitokimia familia piperaceae. Jurnal Biologi dan Pembelajarannya. 7(1): 28–32.

Safitri, I., Wibowo, Y. G., Rosarina, D., and Sudibyo. 2021. Synthesis and characterization of magnetite (Fe_3O_4) nanoparticles from iron sand in Batanghari, IOP Conference Series: Materials Science and Engineering. 1011: 012020.

Saragi, T., Depi, B. L., Butarbutar, S. L., Permana, B., Risdiana. 2018. The impact of synthesis temperature on magnetite nanoparticles size synthesized by co-precipitation method. Journal of Physics Conference Series. 1013(1): 012190.

Strehlow, W.H and Cook, E. L. 1973. Compilation of energy band gaps in elemental and binary compound semiconductors and insulators. Journal of Physical and Chemical Reference Data, 2(1):163-200.

Taib, N. I., Abdul Latif, F., Mohamed, Z., and Zambri, N. D. S. 2018. Green synthesis of iron oxide nanoparticles (Fe_3O_4-NPs) using azadirachta indica aqueous leaf extract. International Journal of Engineering & Technology. 7(4.18): 9–13.

Tauc, J., Grigorovici, R. and Vancu, A. 1966. Optical prpperties and electronic structure of amorphous germanium. Physica Status Solidi (b). 15: 627-637.

Venkateswarlu, S., Natesh Kumar, B., Prasad, C. H., Venkateswarlu, P., and Jyothi, N. V. V. 2014. Bio-inspired green synthesis of Fe_3O_4 spherical magnetic nanoparticles using *Syzygium cumini* seed extract. Physica B: Condensed Matter. 449: 67–71.

Verwey, E. J. W. 1939. Electronic conduction of magnetite (Fe_3O_4) and its transition point at low temperatures [5]. Nature. 144(3642): 327–328.

Yew, Y. P., Shameli, K., Miyake, M., Kuwano, N., Bt Ahmad Khairudin, N. B., Bt Mohamad, S. E., and Lee, K. X. 2016. Green synthesis of magnetite (Fe_3O_4) nanoparticles using seaweed (*Kappaphycus alvarezii*) extract. Nanoscale Research Letters. 11(276): 1-7.

Yusefi, M., Shameli, K., Yee, O. S., Teow, S. Y., Hedayatnasab, Z., Jahangirian, H., Webster, T. J., and Kuča, K. 2021. Green synthesis of Fe_3O_4 nanoparticles stabilized by a *Garcinia mangostana* fruit peel extract for hyperthermia and anticancer activities. International Journal of Nanomedicine. 16: 2515–2532.

Yuvakkumar, R. and Hong, S. I. 2014. Green synthesis of spinel magnetite iron oxide nanoparticles. Advanced Materials Research. 1051: 39–42.

Zhang L, Dong W. F., and Sun H. B. 2013. Multifunctional superparamagnetic iron oxide nanoparticles: Design, synthesis and biomedical photonic applications. Nanoscale. 5(17): 7664–7684.

Zhao, H., Saatchi, K., and Häfeli, U. O. 2009. Preparation of biodegradable magnetic microspheres with poly (lactic acid)-coated magnetite. Journal of Magnetism and Magnetic Materials. 321(10): 1356–1363.

Zhou, Z. H., Wang, J., Liu, X., and Chan, H. S. O. 2001. Synthesis of Fe_3O_4 nanoparticles from emulsions. Journal of Materials Chemistry. 11(6): 1704–1709.

Zulaicha, A. S., Saputra, I. S., Sari, I., and Annas, D. 2020. Synthesis and characterization of modified magnetite (Fe_3O_4) microparticles in the utilization of rust with weeds leaf extract (*Imperata cylindrica* L). Journal Jejaring Matematika Dan Sains, 2(2): 51–55.

OPEN access freely available online
Natural and Life Sciences Communications
Chiang Mai University, Thailand. https://cmuj.cmu.ac.th